Vol. 455: 211–228, 2012
doi: 10.3354/meps09664

MARINE ECOLOGY PROGRESS SERIES
Mar Ecol Prog Ser

Published May 30

Coordinated nocturnal behavior of foraging jumbo squid *Dosidicus gigas*

Kelly J. Benoit-Bird[1,*], William F. Gilly[2]

[1]College of Oceanic and Atmospheric Sciences, Oregon State University, 104 COAS Administration Building, Corvallis, Oregon 97331, USA

[2]Hopkins Marine Station, Department of Biological Sciences, Stanford University, 120 Oceanview Boulevard, Pacific Grove, California 93950, USA

ABSTRACT: We used split-beam acoustic techniques to observe free-swimming of jumbo squid *Dosidicus gigas* during 4 cruises in the Gulf of California. Four-dimensional spatio-temporal data revealed that at night in shallow water, jumbo squid were using ascending, spiral-like swimming paths to emerge from extremely dense aggregations, and were likely foraging on potential prey that were found overlapping in depth with their tracks. Within small regions at the vertices of these swimming paths, individual squid swam back and forth repetitively before continuing their ascent. The behaviors observed in these high-use regions, described using density kernel statistics, are consistent with other observations of prey capture behavior by squid. Often, the observed swimming paths of individual squid were found to parallel those of other squid in depth over time. In addition to being coordinated in depth, movements of individuals within a group of up to 40 individuals were coordinated in horizontal space so that high-use areas were overlapping in horizontal space but separated vertically. The resulting groups of tracks look like interwoven multiple helices anchored at their vertices by bouts of presumed feeding. These highly polarized, complex, coordinated movement patterns constitute schooling. Polarization in these groups did not break down during apparent feeding events as has been observed in other species. In fact, the feeding events themselves may define the anchor for group behavior. Schooling of jumbo squid school will likely be critical in understanding many aspects of their biology.

KEY WORDS: Foraging · Behavior · Squid · Group feeding · Tracking · Schooling · Acoustics · Gulf of California

INTRODUCTION

Many species actively form aggregations, suggesting that this behavior confers an evolutionary advantage (Partridge 1982). The most striking examples of self-organized animal aggregations in the ocean are the discretely bounded schools made up of polarized individuals, i.e. individuals moving in parallel fashion (Pitcher & Parrish 1993), that have been observed in euphausiids (Hamner & Hamner 2000) and more than 50% of fish species at some point in their life histories (Shaw 1978). Because of the ubiquity and conspicuousness of schools of coordinated, polarized individuals and, more generally, socially grouped individuals in shoals, much work has been done to examine the costs and benefits for individuals within these aggregations, particularly in fish. Being part of a group can increase access to mates while reducing an individual's probability of being successfully attacked by a predator through the effects of dilution and confusion of the predator (reviewed by Parrish 1991). Aggregation can increase the likelihood of detecting a predator using the 'many eyes' of the group, resulting in effective anti-predator responses

*Email: kbenoit@coas.oregonstate.edu

(see a review in Pitcher & Parrish 1993). Groups of fish have also been shown to find food faster than individuals (Pitcher et al. 1982) and to dedicate more time to feeding because of a decreased need for predator vigilance by each individual (Magurran et al. 1985). However, being in a group can also increase the intraspecific competition for food (Bertram 1978) and other resources while increasing the probability of agonistic intraspecific interactions (Ruzzante 1994). Thus, it is likely that a balance between predation risk and foraging needs determines the size and structure of animal aggregation.

Aggregation is also important to squids. Many squid species have been observed in both shoals and schools (Hanlon et al. 1979, Nicol & O'dor 1985), foraging (Foyle & O'Dor 1988) or spawning (Hanlon 1998, Smale et al. 2001, Forsythe et al. 2004, Moltschaniwskyj & Pecl 2007). Jumbo or Humboldt squid *Dosidicus gigas*, active pelagic migratory predators that grow to lengths of 2.5 m in total length with weights up to 50 kg, have also been observed in aggregations. These aggregations occur primarily at night when *D. gigas* vertically migrate into near-surface waters to forage on mesopelagic micronekton of the deep-scattering layer that undergo diel vertical migration (Nesis 1970, Gilly et al. 2006). This squid is a true keystone species, transferring energy directly from myctophids, other small mesopelagic fish, crustaceans, and other squid in the deep scattering layer to apex predators such as sperm and pilot whales and the largest fishes (Shchetinnikov 1988). *D. gigas* is also commercially important, supporting the world's largest invertebrate fishery. This fishery is carried out at night when squid are more accessible and perhaps more tightly grouped. Despite this ecological and economic relevance, little is known about natural behavior of *D. gigas* in regard to aggregation. Studies thus far have been largely limited to shipboard observations, tagging of individual squid, and observations using remotely-operated vehicles (Zeidberg & Robison 2007). None of these methods is ideal for studying natural aggregation in such a large, highly mobile, free-swimming squid.

One approach to elucidate the reasons for intraspecific aggregation is to examine how animals organize themselves in space and time. Often, this has taken a static, time-independent approach that ignores how animals move within the group (Partridge 1980, Campbell 1990). However, the movements and interactions of individuals within aggregations can provide insights into the function of the aggregations themselves (Okubo 1986). In fish, descriptions of this kind have been limited by technical challenges because of the need for 4-dimensional (4D) spatio-temporal information (Parrish & Turchin 1997). In this study, we use active sonar tracking to identify aggregations of jumbo squid in the Gulf of California and elucidate what individuals do within aggregations. Collection of 4D data on individual squid in- and outside of groups over many short time periods revealed a novel behavior that may underlie a general foraging strategy in this species.

MATERIALS AND METHODS

Acoustic data and squid samples were collected around the clock in the central Gulf of California, throughout the triangular area bounded by 28.93 N, 113.34 W; 27.79 N, 110.60 W; 26.98 N, 112.24 W (Fig. 1), during 4 cruises. The dates for each cruise, the platforms and transducers used, and Simrad EK60 settings are shown in Table 1. Continuous acoustic sampling with multi-frequency echosounders was carried out throughout each cruise with a sampling rate of 4 to 10 Hz. During each cruise, the echosounders were calibrated using a 38.1 mm diameter tungsten carbide reference sphere (Foote et al. 1987). Acoustic sampling while the vessel was stationary was conducted periodically throughout each cruise and was frequently accompanied by efforts to

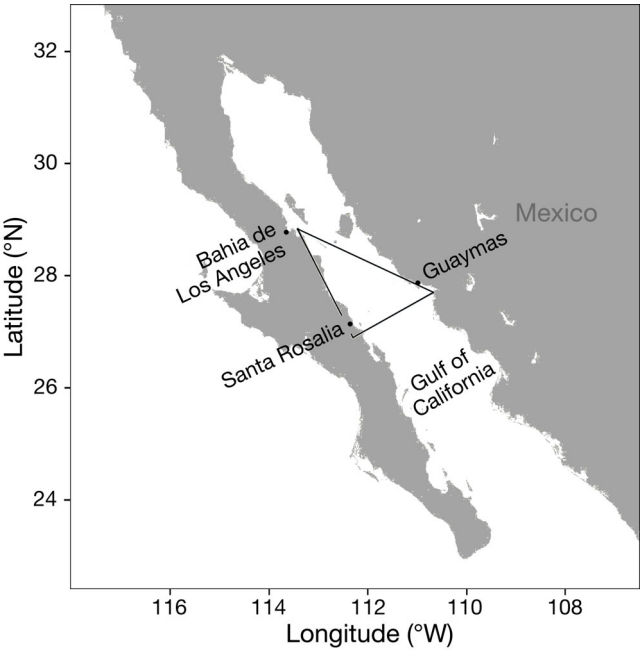

Fig. 1. Sampling area (black triangle) in the Gulf of California, where acoustic data and samples of jumbo squid *Dosidicus gigas* were collected by 4 research cruises between 2007 and 2011

Table 1. Summary of research cruises undertaken in the Gulf of California to collect acoustic data and samples of jumbo squid *Dosidicus gigas*, showing the echosounders used and their settings. During all 4 cruises, temperatures at depths of 50–100 m were similar with overall mean values (±SD) of 18.4ºC (2.11) at 50 m and 15.6ºC (1.1) at 100 m. Surface temperatures in November and June averaged 24.1ºC (1.8) in November and June and 19.3ºC (0.8) in March. PL: Pulse length

Dates	Platform	Transducer		38 kHz		70 kHz		120 kHz		200 kHz	
		Depth (m)	Location	PL (µs)	Beam	PL (µs)	Beam	PL (µs)	Beam	PL (µs)	Beam
17–27 Mar 2007	RV 'Pacific Storm'	1	Pole	1024	12° split	512	7° split	256	7° split	256	7° split
11–20 Nov 2008	RV 'BIP XII'	3	Hull	1024	15° single	–	–	256	7° split	–	–
3–15 Jun 2010	RV 'New Horizon'	1	Pole	512	12° split	512	7° split	512	7° split	512	7° split
9–22 June 2011	RV 'New Horizon'	1	Pole	512	12° split	512	7° split	512	7° split	512	7° split

capture jumbo squid via weighted, luminescent jigs and occasionally, surface dip netting. During each jigging session, a minimum of 20 squid were caught for measurements unless this required more than 1 h of effort. Dorsal mantle length and total mass were measured for each captured squid. After these measurements were completed, the squid was euthanized by rapid decapitation, and sex and maturity stage were determined (Lipinski & Underhill 1995), and the major, undigested contents of the stomach were identified visually as described elsewhere (Markaida et al. 2008).

All 5-min intervals during which the vessel was stationary, and when squid had been caught by jigging within the previous or subsequent 2 h, were candidates for inclusion in the analysis. These criteria resulted in a total of 87 h of acoustic samples of 1040 5-min intervals. Because of the bias in jigging which was primarily successful at night when squid were closer to the surface, we focused on intervals sampled during the period between just before sunset and just after sunrise. The number of stationary sampling intervals was split roughly evenly among cruises in 2007, 2010, and 2011. In 2008, about double the number of sampling intervals of other years met the criteria for inclusion. From the candidate sampling periods, 100 non-adjacent 5-min intervals were randomly selected.

Only data between 2.5 and 400 m below the transducers were included in the analysis. The volume scattering data from all available frequencies in the selected time intervals was compared by subtracting each frequency from the 38 kHz data. Areas that had scattering at least 3 dB greater at 120 kHz than at 38 kHz were categorized as small scatterers, i.e. animals that could serve as squid prey. The median depth and the depth of the peak (e.g. maximum intensity) of this scattering for each 5-min interval were determined. Areas that had values at least 3 dB greater at 38 kHz than at all other frequencies, consistent with the frequency expected for jumbo squid (Benoit-Bird et al. 2008), were retained for squid analysis. In areas with high densities of squid targets, volume scattering was analyzed using echo-energy integration using the mean target strength expected based on the length distribution of squid captured at approximately the same time.

Single targets, e.g. only 1 target per acoustic reverberation volume for each pulse (Sawada et al. 1993), were extracted using Myriax's Echoview 5.0 program from the remaining 120 kHz echosounder data to a depth of 400 m. The single target detection criteria were based on those presented in Benoit-Bird et al. (2008), which were empirically confirmed. Single targets could be localized with 10 cm of resolution in the horizontal plane and 5 cm in the vertical plane.

Groups of single targets that showed a pattern of systematic movement in 4 dimensions were identified as tracks using the split-beam capabilities of the 120 kHz echosounder on all the research platforms utilized. To identify these tracks, the tracking algorithm in Echoview was utilized, and this assumed that targets grouped into a track were generated by a single object moving through space. This algorithm is based on the fixed-coefficient filtering method for radar target tracking following Blackman (1986) and incorporates vessel motion to allow the real position of the target to be localized (Handegard et al. 2005). For analysis, single target thickness was defined as half the pulse length to maximize the vertical resolution of the data. The sensitivity of the tracker to unpredicted changes in position and velocity in the horizontal plane were defined as 1 and 0.75, respectively. Sensitivity for changes in vertical position and velocity were set to 0.25 and 0.05. Thus, the detector was more responsive to target motion in the horizontal plane than the vertical. This is consistent with what is known about the swimming patterns of jumbo squid from tagging data (Gilly et al. 2006) as well as the patterns observed in individual targets likely to be squid and found in uncluttered habitats where tracks were not likely to overlap with those of other individuals.

Targets detected in successive pings could be included in a track if they were no more than 10 m apart in the horizontal plane and no more than 0.5 m in the vertical. Each target had to be separated by less than 10 pings. The horizontal distance allowed between successive detections was permitted to increase by 5 m for each successive ping in which the target was not detected but by only 0.025 m in the vertical for each missed ping. Targets that were considered candidates for a given track based on their position were then either selected or rejected for inclusion based on these position characteristics as well as their target strength relative to other targets in the track. These factors were weighted in the selection process (major axis 0.05, minor axis 0.05, target range 0.52, target strength 0.32, ping gaps 0.05). Each target was allowed to be added to only one track. All tracks within each randomly selected 10-min interval were identified. The full duration of each track was included even if it crossed the time interval boundaries. After automatic detection, each track was visually inspected for obvious errors; automatically detected tracks compared well with those identified visually in echograms and a variety of track characteristics were measured (Table 2).

Analysis of individual tracks

For each target detection in a given track, the time of the detection, the depth, latitude, and longitude of the target, and its target strength were extracted. Using these data, the straight-line (e.g. minimum) velocity of the target between successive detections was measured in the horizontal and vertical dimensions as well as in 3 dimensions. Using a 5-point running calculation, tortuosity was calculated as the sum of the distances between 5 adjacent detections in a

Table 2. *Dosidicus gigas.* Summary of variables measured for analysis of jumbo squid tracks

Variable	Description
All tracks	
Trajectory	Categorical descriptor based on the pattern of depth changes over time
Velocity	Swimming speed estimate based on straight-line movements between detections in horizontal, vertical, and 3D space
Tortuosity	The amount of turning in a track; has been used to distinguish behavioral states, e.g. searching vs. foraging
No. of detections	The number of points making up an individual track
Mean track depth	Weighted depth of a detected individual squid
Target strength	The acoustic reflection strength on a logarithmic scale of a single squid corrected for its location in the beam
Scattering strength	A linear measure of acoustic target strength often used as a proxy for animal length, i.e. mantle length in the case of squid
Tracks with upwards movement (tracks at least 25 s in duration with at least 3 m upward movement during some part of the track). All of the variables above, plus:	
Mantle length	Estimated from mean scattering strength (see Benoit-Bid et al. 2008)
Turning angle between successive detections	Describes the squid's swimming path; has been used as an indicator of behavior
95% kernel	Horizontal area covered by a track
95% kernel equivalent circular diameter	Horizontal scale of each track
25% kernel	Highlights areas of high-use/long residence within tracks in horizontal space
25% kernel equivalent circular diameter	Horizontal scale of high-use areas
Distance between centroids of 25% kernels	Separation between high-use areas
Turning angle between 25% kernels	Describes the overall swimming path of the squid
Groups of tracks (temporally overlapping tracks of at least 25 s in duration with similar depth trajectories and a depth separation between pairs of tracks <5 m). All of the 2 sets of variables above, plus:	
95% kernel for the group of tracks	Horizontal area covered by simultaneously detected tracks
% overlap of individual and group 95% kernels	Degree of horizontal coincidence of tracks within a group
% overlap of individual 25% kernels in horizontal space	Degree of horizontal coincidence of high-use areas amongst tracks in a group
% overlap of individual 25% kernels in vertical space	Degree of vertical coincidence of high-use areas amongst tracks in a group

track (that is, the total distance traveled) divided by the straight-line distance between the first and last targets of those 5 detections. Tortuosity was also calculated for each track using the total distance traveled during the track and the straight-line distance between its 2 ends. Tortuosity measures how much the squid is turning and is often used in animal tracking studies to describe animal movement paths and to distinguish between behavioral states, e.g. searching and foraging (Morales et al. 2004).

Detected tracks were categorized based on their depth trajectory. Tracks were classified as upward or downward if their depth changed unidirectionally by at least 3 m over the length of the track. If a track varied by less than 3 m in depth, it was categorized as a horizontal track. If a track varied by more than 3 m in depth but changed vertical direction during tracking, it was categorized as undulating. Because of a large discrepancy in the number of tracks of each type detected, 150 tracks of each type were randomly selected for statistical analysis of track-type effects. The effect of track type on the total number of targets within a track (no. of detections), mean track depth, mean and maximum 3D velocity, mean scattering strength (σ^2), standard deviation of σ^2, target strength range, and total track tortuosity were examined using a multivariate analysis of variance (MANOVA) followed by post-hoc analysis using Dunnett's C tests, which provide an estimate of the mean difference ($\bar{\Delta}$) of effects between track types as well as the 95% confidence interval (CI) about this mean. The primary goals of this analysis were to determine if all types of tracks were equally likely to be detected and if individual scattering strength, a linear measure of target strength, is robust to changes in animal orientation and thus can be used to accurately estimate mantle length under field conditions.

The 150 randomly selected undulating tracks were further examined to determine if scattering strength was affected by changes in track trajectory, again to determine if this is a reliable proxy for mantle length. These tracks were split into segments of 10 detections or longer that could be categorized as upward, downward, or horizontal tracks. A repeated measures analysis of variance (ANOVA) was used to determine if there was a significant effect of trajectory on backscattering strength.

Tracks with upward movement

For tracks with at least 3 m movement upwards during some part of the track, e.g. upward tracks and most undulating tracks that were at least 25 s in duration (sample shown in Fig. 2), additional analyses were conducted. The mean target strength (averaged in the linear domain) for each track was used to estimate the mantle length of each target following Benoit-Bird et al. (2008). Mean mantle length of squid tracked within a 5-min interval was compared to the mean mantle length of squid captured via jigging at the same location within 2 h of the sample interval using regression analysis. This allowed inclusion of all of the stationary periods of the research vessel, increasing the sample size; despite the relatively wide time interval allowed for comparison, more than half of the 5-min intervals included coincided directly with jigging efforts. The average depth of each of these tracks was compared to the median depth of small scatterers in the upper 400 m of the water column as well as the depth of the peak scattering from small scatterers at 120 kHz during the same 5-min interval as the track, using regression.

The horizontal use of habitat by each tracked individual was described using adaptive kernels that had been optimized by least-squares cross validation (Worton 1989). Cells in the analysis grid were held constant at 0.1 m. The 95% utilization contour was used to define the horizontal area covered by each track. The 25% utilization contour was used to define areas of high habitat use. The 25% kernels of each of the 3 sample tracks from Fig. 2 are shown in gray overlaying each track in Fig. 3. The equivalent circular diameter of the 25% utilization area was used to describe the scale of these high-use areas. The distances and angles between the centroids of these areas were used to describe the average horizontal swimming path used by each squid. Turning angle is a parameter in many movement models and is frequently used to describe animal movement, with most directed movement having low angle values and search indicated by high values (Turchin 1991). The relationship between squid mantle length estimated from target strength and these variables as well as velocity and tortuosity of the track were explored using regression analysis. A MANOVA with repeated measures was used to determine if there were differences in horizontal, vertical, and 3D velocity, turning angle between successive detections, tortuosity, and the standard deviation of these measures between high-use areas (the 25% kernels), and the remainder of each track split into segments with upward or downward trajectories. Dunnett's C post-hoc analysis was used to identify specific differences.

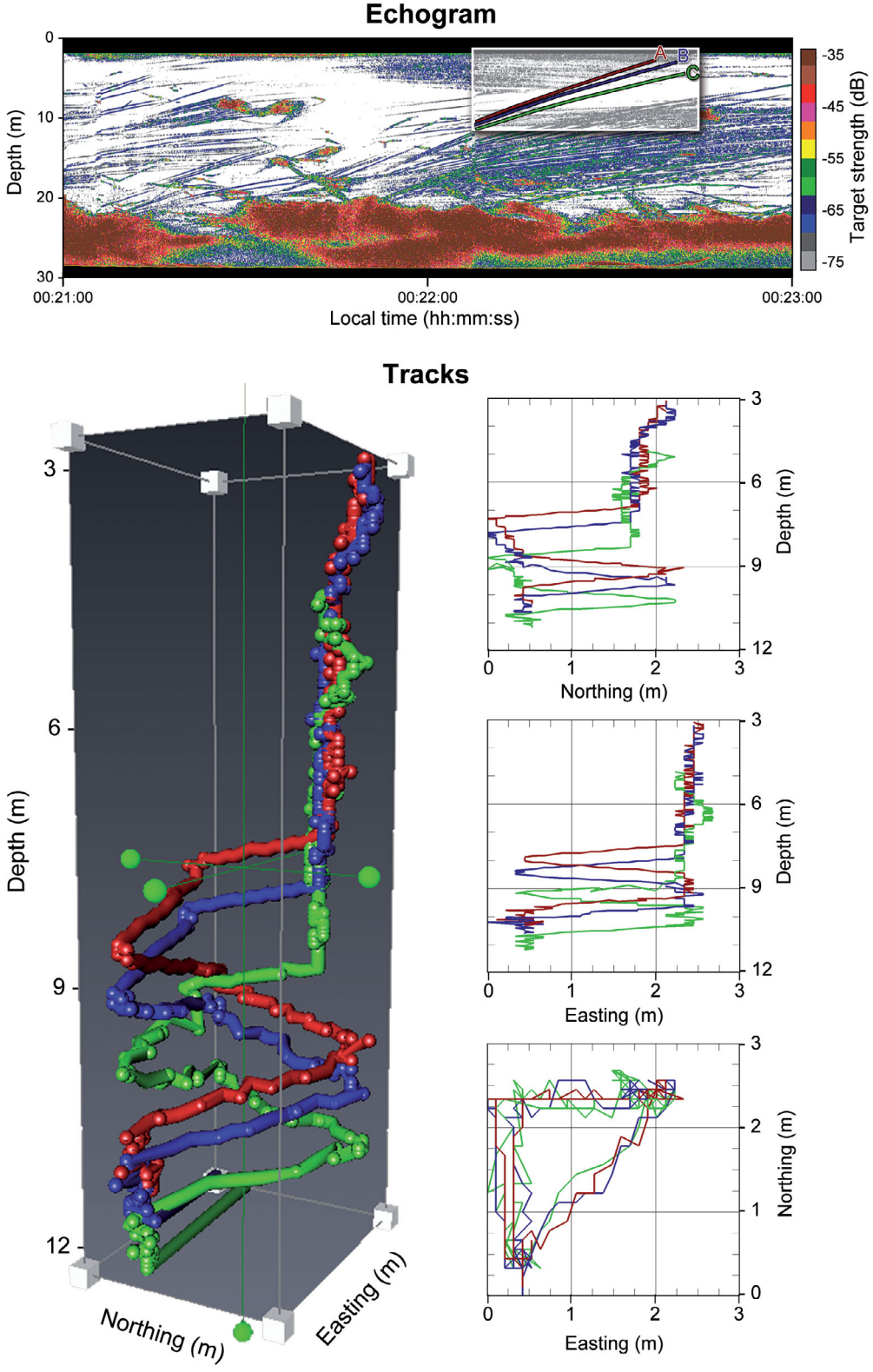

Fig. 2. *Dosidicus gigas*. An example of 3 simultaneously detected tracks (A: red; B: blue; C: green). The top panel shows the 120 kHz echogram. The tracks of 3 individual squid are highlighted. The mean target strength of each track was approximately −42 dB when corrected for position in the beam. The 3D locations of these 3 tracks are shown relative to their own origin (bottom left), and in each 2D plane (bottom right)

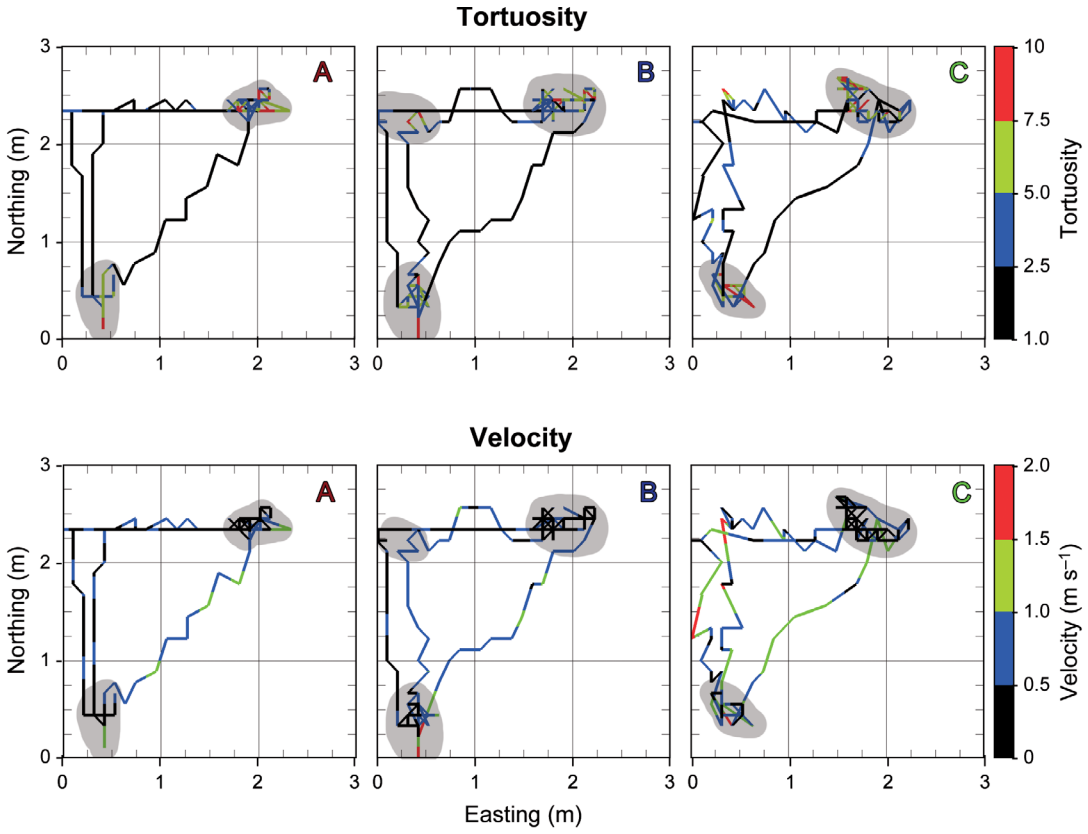

Fig. 3. *Dosidicus gigas.* Tortuosity (top panels), a measure of the amount of turning in a track, and instantaneous 3D velocity (bottom panels) for the 3 sample tracks A, B and C from Fig. 2. Areas of high habitat use (25% kernels) are shaded gray

To examine the effects of prey type and cruise on track characteristics, 10 tracks were randomly selected from each 10-min interval included in the analysis. The numerically dominant prey group, determined by analysis of stomach contents from captured squid, was classified as euphausiids (N = 31), myctophids (N = 30), other fish (N = 28) or 'other', which included pteropods, other crustaceans, and assorted squid (N = 11). A MANOVA was then used to examine the effects of the dominant prey and cruise on track characteristics. Bonferonni post-hoc analysis was conducted for variables that showed significant effects.

Groups of tracks

Temporally overlapping tracks of at least 25 s in duration with similar depth trajectories and a depth separation between pairs of tracks ≤5 m were defined as a group. An example of 3, simultaneously detected tracks is shown in Fig. 2. For grouped tracks, the distance between adjacent individuals was measured in the horizontal plane, in the vertical, and in 3D space for every echo in which the 2 individuals were detected. The effect of squid mantle length and differences in mantle length between individuals on these measures was explored using regression.

The relationship between the mean turning angle connecting the 25% kernels for tracks in the same group was analyzed using a repeated measures ANOVA, treating each track in a group as a replicate to determine if individuals in a group had a shared swimming pattern. To measure the degree of overlap between tracks in a group, a single 95% density kernel was calculated for the simultaneously detected tracks and the percent overlap of the 95% kernels of each individual track was compared to the 95% kernel for the entire group of simultaneously tracked individuals. The percent overlap of the 25% kernels of all simultaneously tracked individuals was also calculated to determine how similar the high-use areas were within a group. The overlap of the example tracks from Fig. 2 is shown in Fig. 4. To determine if this overlap was greater than expected by chance, the area covered by each track's 25% kernel was divided by the area covered by the 95% kernel for

the group and then these were multiplied together to determine the overlap expected from multiple, randomly moving squid in the same area. A 2-sample Kolmogerov-Smirnov test was used to determine if the distribution of the overlap between the 25% kernels was significantly different than the distribution of overlap predicted by chance.

The overlap of the 25% kernels defined in the horizontal plane was also examined in the vertical dimension. The percent of vertical overlap of tracks within these 25% kernels was compared to the overlap expected by chance. The chance prediction was calculated as the depth range of each track within its kernel divided by the total depth range over which the tracks overlap multiplied by the same calculation for all other tracks in the group. This calculation was repeated using only the area in which all of the 25% kernels for the whole group overlap. Both values were examined with Kolmogerov-Smirnov tests to determine if the distribution of the vertical overlap between the high-use areas of individuals was different than the distribution of overlap predicted by chance. In addition, for co-detected groups of 4 or more individual tracks, similar pairwise examinations were done of the vertical and horizontal overlap and regression analysis was used to examine possible relationships between overlap in the 2 different dimensions.

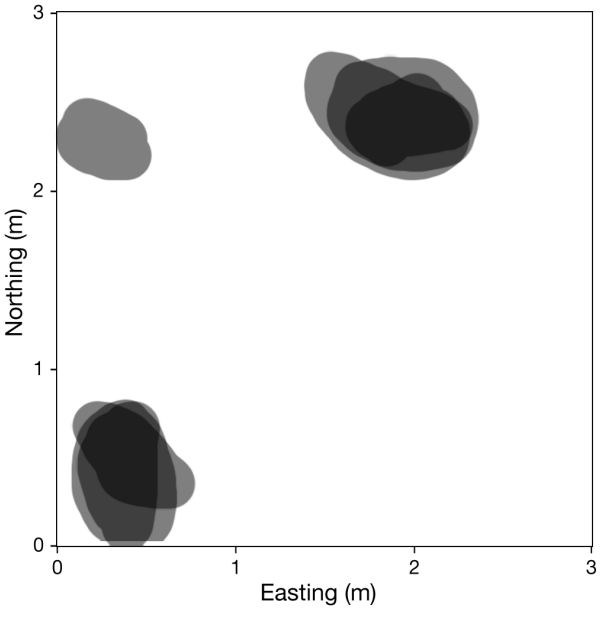

Fig. 4. *Dosidicus gigas.* The 25% kernels from the tracks in Fig. 2 superimposed to show the overlap. The darkest color shows the area in which all 3 tracks overlap; representing 38% of the total area of the three 25% kernels and being a measure of the degree of horizontal coincidence amongst these 3 tracks. If only the 2 kernel areas where all 3 squids were identified are included (the northeastern kernels and the kernels near the origin), the complete overlap between the 3 squids' 25% kernels increases to 45%

The characteristics of solitary squid tracks were compared to tracks found in groups. Because of the correlations between tracks found simultaneously, one track was randomly selected from each group for this comparison. Analysis of variance was used to determine if there was a significant effect of grouping on the track's average tortuosity and average horizontal, vertical, and 3D velocity, the 25% kernel diameter, 95% kernel diameter, tortuosity in and between 25% kernels, the turning angle between 25% kernels, and the calculated length of the target. In addition, the relationship between the density of squid in the aggregation below each track or group of tracks to the number of squid tracked simultaneously was explored using regression.

RESULTS

A total of 143 127 tracks were detected, all in the upper 90 m of the water column, with 90% in areas where the bottom was 75 m or shallower. The median depth of detected tracks was 34 m. These tracks averaged 11 s in duration, or 40 points, with the longest track covering 139 s and 648 points. Of these tracks, 103 763 had upward trajectories, 164 had downward trajectories, 39 012 had an undulating depth pattern, and 188 did not change in depth over time.

MANOVA was used to examine the effects of track trajectory type on track characteristics. This analysis showed that there was no significant effect of track type on the target's scattering strength, the standard deviation of this measure, or the range in target strength values measured within a track (F = 1.04, 0.86, and 0.44, respectively; df = 3, 596; $p > 0.05$ for all comparisons), indicating that target strength is not affected by changes in squid behavior within a track. There was a significant effect of track type on the number of targets detected within the track ($F = 8.28$, $p < 0.001$), mean track depth (F = 7.84, $p < 0.001$), mean velocity ($F = 3.30$, $p < 0.05$), and track tortuosity (F = 7.96, $p < 0.001$). Post-hoc analyses revealed that most differences were found in the downward tracks, which had significantly fewer target detections per track than all other track types ($\bar{\Delta}$ = 91, 95% CI 40 to 142), were found an average of 15 m shallower than other track types (95% CI 4 to 27 m), and had an average velocity 0.82 m s^{-1} faster than all other track types (95% CI 0.08 to 1.56 m s^{-1}; Dunnett's C $p < 0.05$ for all comparisons). Analysis of track tortuosity showed that the only significant difference between

track types was for horizontal tracks which had a significantly higher total track tortuosity than the other track types ($\bar{\Delta}$ = 8 m, 95% CI 2 to 15, $p < 0.05$)

The 150 randomly selected undulating tracks were split into segments that could be categorized as upward, downward, or horizontal and analyzed with a repeated measures ANOVA. This analysis showed a significant between-track effect on backscattering strength ($F = 5912$; df = 1, 599; $p < 0.05$) but no within-track effect ($F = 0.91$; df = 2, 599; $p > 0.05$). As a result of the robustness of measurements of target strength to changes in squid swimming orientation, target strength is converted to mantle length for remaining analyses.

Tracks with upward movement

A total of 15 703 tracks greater than 25 s in duration with some upward movement during the track were detected; 9871 of these tracks were entirely upward. In the remaining tracks, the upward components of tracks made up the majority of each observation. In tracks with a downward component, the downward trajectory occurred at the end of individual tracks and comprised less than 10% of each track's duration. Captured squid had mantle lengths that ranged from 4.0 to 84.5 cm. The mean mantle length predicted acoustically from each of the one hundred 5-min intervals was compared to the mean mantle length from squid caught at around the same times. These 2 variables were positively correlated ($R = 0.83$, $p < 0.05$, df = 99), the slope of the line was not significantly different from 1 ($F = 0.62$, $p > 0.05$), and the intercept was approximately zero.

All of the individual tracks detected were found above intense aggregations of scattering consistent with groups of densely aggregated squid. Echo energy integration estimates of the numerical density of squid within these aggregations varied from 3 to 18 squid m^{-3}. There was a significant effect of the median depth of 120 kHz scattering from small scatterers on the mean depth of individual tracks ($R^2 = 0.32$, $p < 0.05$, track depth = 1.86 × median depth − 3.81). There was also a significant effect of the depth of peak scattering from small scatterers on the mean depth of individual tracks ($R^2 = 0.52$, $p < 0.01$, track depth = 0.97 × peak scattering depth + 0.05).

There was no significant effect of squid mantle length on the equivalent circular diameters of the 25% ($R^2 = 0.002$, $p > 0.05$) or 95% kernels ($R^2 = 0.03$, $p > 0.05$), the distances between the centroids of the 25% use areas ($R^2 = 0.06$, $p > 0.05$), the angle between these centroids ($R^2 = 0.09$, $p > 0.05$), or the tortuosity of the track ($R^2 = 0.01$, $p > 0.05$). The mode horizontal size of the high-use areas was 0.5 m (Fig. 5a) while the mode horizontal size of the entire track was approximately 3.5 m (Fig. 5b). The mode of the distances measured between the centroids of the 25% kernels in each track was around 3 m (Fig. 5c) which were separated by an angle of either 60° or 180° (Fig. 6c). There was a significant effect of squid size on the maximum velocity measured in each track ($R^2 = 0.42$, $p < 0.001$; Fig. 7b) but no effect of squid size on the average velocity within each track ($R^2 = 0.0001$, $p > 0.05$; Fig. 7a).

A MANOVA with replication (df = 2, 15 702) showed that there were significant differences in vertical velocity ($F = 3.11$, $p < 0.05$), the standard deviation of horizontal velocity ($F = 7.92$, $p < 0.01$), the standard deviation in 3D velocity ($F = 4.88$, $p < 0.01$), tortuosity ($F = 36.58$, $p < 0.001$), the standard deviation of tortuosity ($F = 84.70$, $p < 0.001$), turning angle between successive detections ($F = 117.36$, $p < 0.001$; Figs. 6a,b), and standard deviation of turning angle ($F = 282.18$, $p < 0.001$), but no significant differences in horizontal velocity ($F = 0.65$, $p > 0.05$), 3D velocity ($F = 0.91$, $p > 0.05$), or the standard deviation of vertical velocity ($F = 0.34$, $p > 0.05$) between high-use areas (the 25% kernels), the ascending components, and descending components of the remainder of the track. Post-hoc analysis using Dunnett's C revealed that the downward components of tracks had higher vertical velocities than the 25% kernels or the other upward segments of each track ($\bar{\Delta}$ = 0.91 m s^{-1}, 95% CI 0.62 to 1.88 m s^{-1}, $p < 0.05$). The 25% kernels had greater standard deviations of horizontal and 3D velocities ($\bar{\Delta}$ = 3.63, 95% CI 1.88 to 6.29), higher tortuosity ($\bar{\Delta}$ = 4.16, 95% CI 2.56 to 10.18), higher standard deviation of tortuosity ($\bar{\Delta}$ = 6.81, 95% CI 1.71 to 11.62), higher mean turning angle ($\bar{\Delta}$ = 84°, 95% CI 37 to 174), and greater standard deviation in turning angle ($\bar{\Delta}$ = 58.52, 95% CI 13.81 to 107.53) than both the upward and downward segments of the remainder of each track ($p < 0.05$ for all comparisons). The example tracks shown in Figs. 2 and 3 illustrate these differences.

A multivariate Pillai's trace statistic showed no significant effect of cruise on the track characteristics measured ($F = 0.49$; $p > 0.05$; df = 39, 222), a significant effect of dominant prey type ($F = 0.77$; $p < 0.01$, df = 39, 222), and no significant interaction between cruise and prey ($F = 1.02$; $p > 0.05$; df = 117, 720) although an ANOVA showed there was a significant effect of cruise on dominant prey ($F = 394.59$; $p < 0.001$; df = 3, 96). The results of the MANOVA showed prey type significantly affected the 95% kernel diameter ($F = 4.12$; $p < 0.05$; df = 1, 84), the dis-

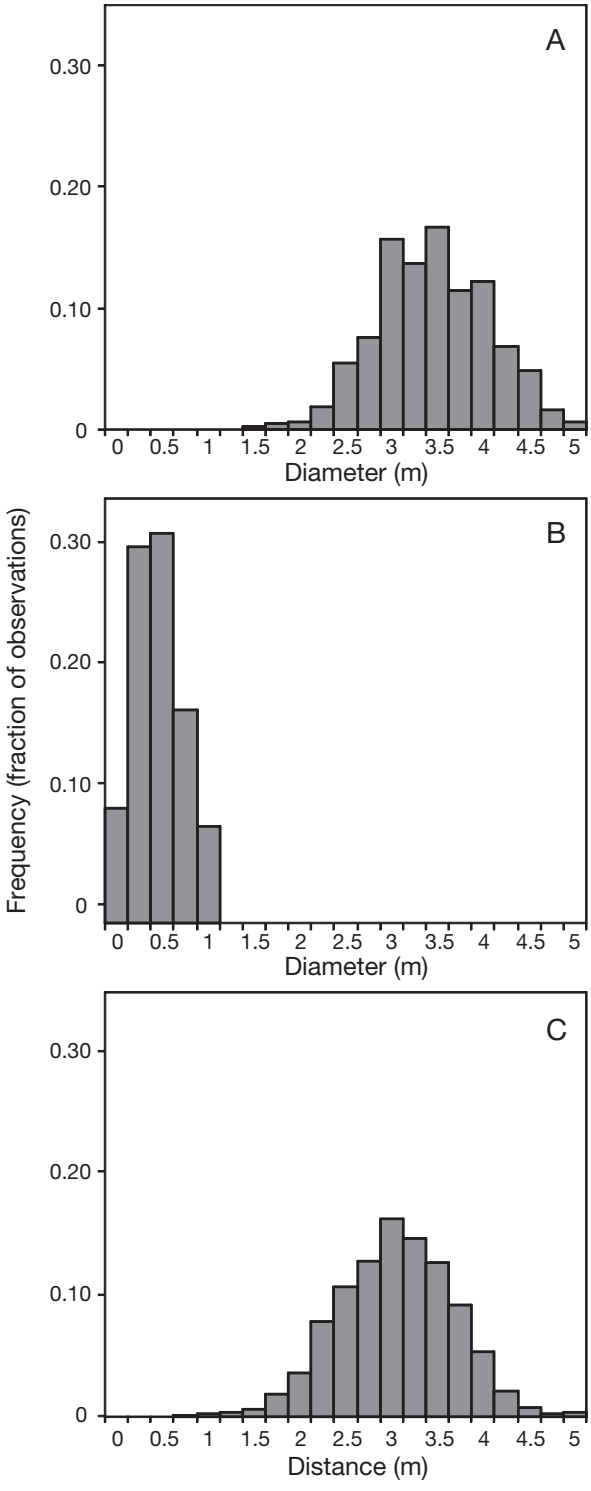

Fig. 5. *Dosidicus gigas*. The distributions of kernel characteristics for all tracks that were at least 25 s long and had some components with an upward trajectory (N = 15 703). (A) 95% kernel equivalent circular diameter, a measure of the horizontal scale of each track. (B) 25% kernel equivalent circular diameter, a measure of the horizontal scale of high-use areas within each track. (C) Distance between 25% kernel centroids, i.e. the separation between these high-use areas

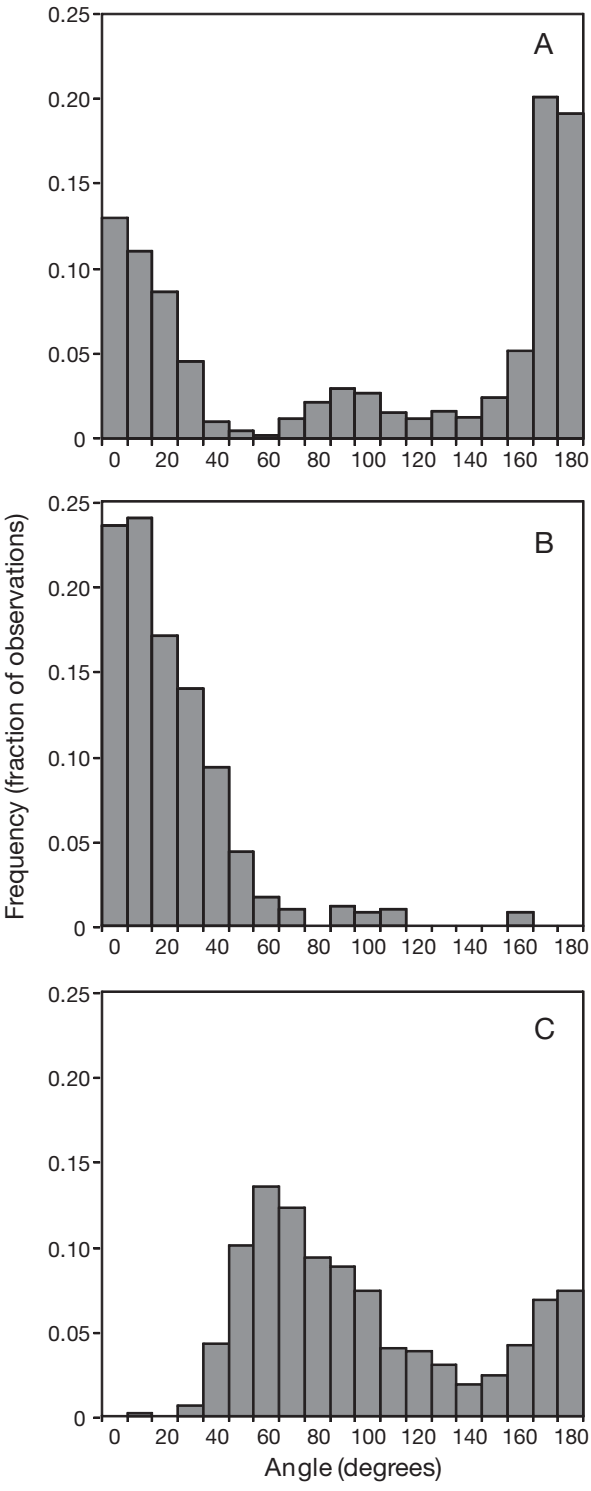

Fig. 6. *Dosidicus gigas*. The distributions of turning angles, a descriptor of the swimming path and behavioral state, for all tracks that were at least 25 s long and had some components with an upward trajectory (N = 15 703). (A) Turning angle between detections inside the 25% kernels. (B) Turning angle between detections outside 25% kernels. (C) Angle between centroids of the 25% kernels

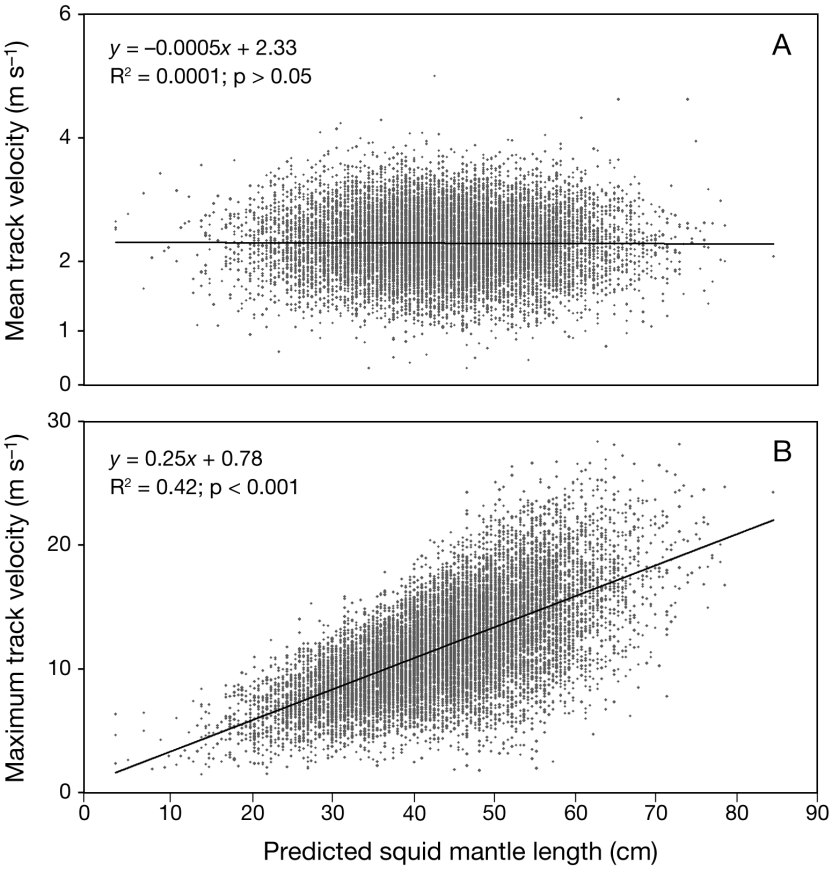

Fig. 7. *Dosidicus gigas.* The relationship between squid mantle length predicted from target strength and (A) the mean and (B) the maximum 3D velocity for each track

tance between 25% kernel centroids (F = 3.32; p < 0.05; df = 1, 84), and the 3D velocity within 25% kernels (F = 4.08; p < 0.05; df = 1, 84) but no significant effect on other track characteristics. Post-hoc analysis showed that the tracks of individuals during times when squid contained primarily euphausiids had significantly smaller 25% kernels ($\bar{\Delta}$ = 0.09, 95% CI −0.02 to +0.21), shorter distances between 25% kernel centroids ($\bar{\Delta}$ = 0.42, 95% CI −0.05 to +0.64), and were slower within the 25% kernels ($\bar{\Delta}$ = 0.33, 95% CI 0.18 to 0.42) than other tracks.

Groups of tracks

Multiple 25 s or longer tracks were often observed overlapping in time with similar depth trajectories and a depth separation of 5 m or less. In these 9429 tracks in 2975 groups of up to 40 individuals, there was always significant upward movement as shown in Fig. 2 for 3 simultaneously detected tracks and Fig. 8 for a group of 20 simultaneously detected tracks. The minimum distance between neighboring individuals within a group was measured in the horizontal plane, in the vertical, and in 3D space for every echo in which both individuals were detected. The minimum horizontal distance between individuals remained between 0.1 and 0.2 m, regardless of squid mantle length or the difference in length between the 2 individuals. The minimum 3D distance was thus controlled by the vertical separation of individuals and could be considered equivalent because of their nearly perfect correlation, so only 3D distance was considered. There was no significant relationship between the average length of the 2 squid measured and their minimum 3D separation distance (R^2 = 0.02, p > 0.05). The difference in squid mantle lengths did affect 3D separation distance (R^2 = 0.14, p < 0.05); however, this relationship was best described by expressing the difference in length as a percent of the smaller squid's length, resulting in a positive linear relationship between the 2 variables (R^2 = 0.37, p < 0.01, N = 6454; Fig. 9).

A repeated measures ANOVA showed that there was a significant difference between groups of tracks on the mean turning angle connecting the 25% kernels (F = 93.28; df = 1, 9428; p < 0.05) but no significant difference within a group (F = 1.64; df = 1, 9428; p > 0.05). The overlap of each 95% kernel in a group and the 95% kernel for the entire group is shown as a function of the number of co-detected tracks in Fig. 10a. The horizontal overlap of the 25% kernels is shown in Fig. 10b. This overlap was significantly greater than that predicted by chance (D = 0.76, p < 0.001, N = 6454). The overlap of the 25% kernels defined in the horizontal plane was also examined in the vertical dimension. The overlap was significantly less than that predicted by chance using both the entire depth over which the group of tracks overlapped (D = 0.53, p < 0.01, N = 6454; Fig. 10c) and only the overlap within the 25% kernels (D = 0.58, p < 0.01, N = 6454). For co-detected groups of 4 or more individual tracks, the relationship between horizontal and vertical overlap of each pair in the group is shown in Fig. 11. There was a significant, negative linear relationship between the overlap in the 2 planes (R^2 = 0.38, p < 0.05).

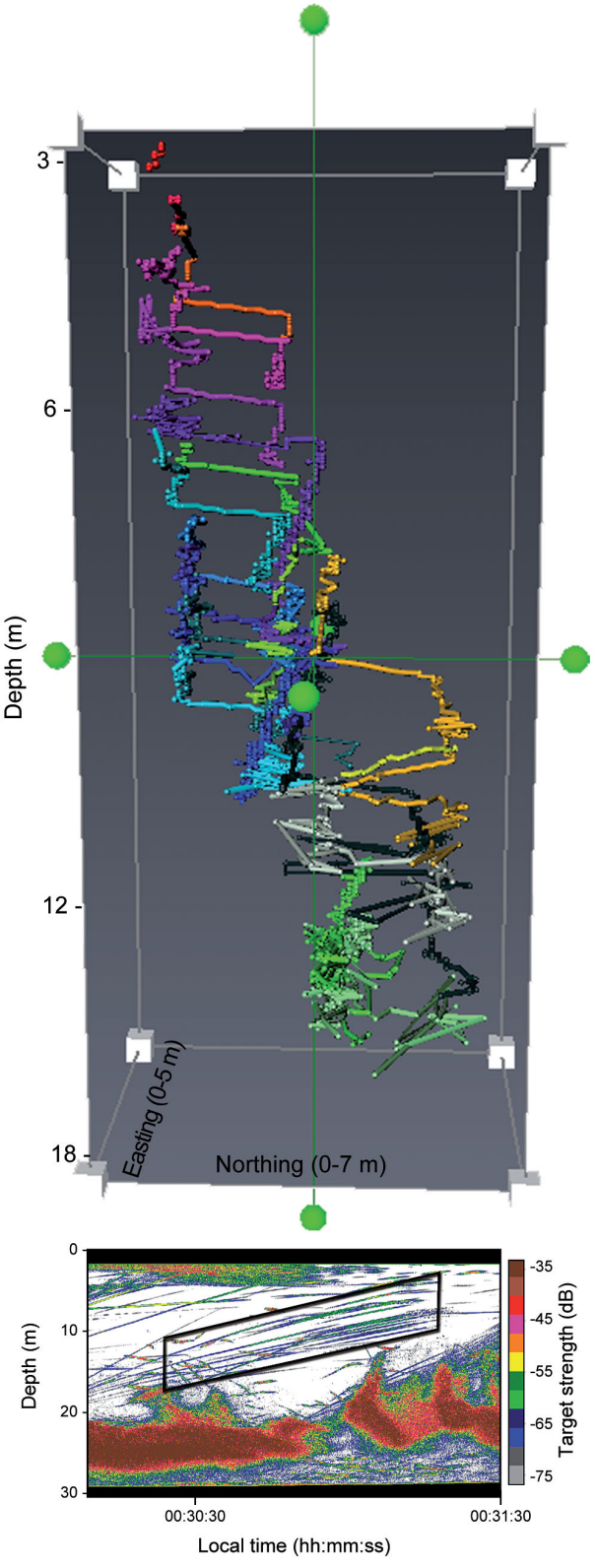

Fig. 8. *Dosidicus gigas.* An example of tracks from a group of 20 simultaneously detected individuals. The upper panel shows the 3D position of each track in a different color. The bottom panel shows the 120 kHz echogram. The region of the tracks is outlined in black. The mean target strength of each track corrected for beam effects ranged from –53.1 to –49.3 dB

The characteristics of solitary squid tracks were compared to tracks found in groups using MANOVA (df = 1, 9247). There was no significant effect of grouping on the 3D velocity ($F = 0.74$, $p > 0.05$), 25% kernel diameter ($F = 0.01$, $p > 0.05$), tortuosity in 25% kernels ($F = 0.83$, $p > 0.05$), turning angle between 25% kernels ($F = 1.73$, $p > 0.05$), or target length ($F = 1.38$, $p > 0.05$). There was a significant effect of grouping on the average tortuosity of each track ($F = 17.10$, $p < 0.05$), the tortuosity between 25% kernels ($F = 26.38$, $p < 0.05$), the horizontal velocity ($F = 34.45$, $p < 0.01$), the vertical velocity ($F = 110.04$, $p < 0.01$), and the 95% kernel diameter ($F = 28.22$, $p < 0.05$). Solitary tracks were more tortuous overall ($\bar{\Delta} = 0.72$, 95% CI 0.02 to 1.21), had higher tortuosity in the track segments between 25% kernels ($\bar{\Delta} = 0.24$, 95% CI 0.06 to 0.91), had faster horizontal velocities ($\bar{\Delta} = 0.47$, 95% CI 0.09 to 1.17), slower vertical velocities ($\bar{\Delta} = 0.61$, 95% CI 0.04 to 1.48), and larger 95% kernel diameters than tracks in groups ($\bar{\Delta} = 0.48$ m, 95% CI 0.11 to 1.06). There was a significant, positive, linear relationship between echo energy integration estimates of the numerical density of the squid aggregations below tracked individuals and the number of squid tracked simultaneously ($R^2 = 0.43$, $p < 0.01$).

DISCUSSION

Two types of aggregations

At night, squid in shallow water were found in 2 distinct types of aggregations during cruises in 4 different years: extremely dense groups in which individual squid could not be acoustically localized, and looser, highly coordinated groups of several individuals (up to 40) following parallel paths upwards from the dense groups (Figs. 2 & 8). These 2 dramatically different aggregation types indicate different drivers for aggregation at the same time and location. Only the tracked squid leaving these aggregations in smaller, less dense groups overlapped well with acoustic targets that were consistent with potential prey. These squid were also at depths targeted by jigging efforts as the line could rarely be lowered to the deeper aggregations without capturing an individual at shallower depth. The squid captured had fresh, identifiable food in their stomachs. Together, these data suggest a foraging function for these looser aggregations of jumbo squid leaving denser masses, similar to observations of *Illex illecebrosus* leaving dense schools in order to forage (Foyle & O'Dor 1988). The loose groups in which individual

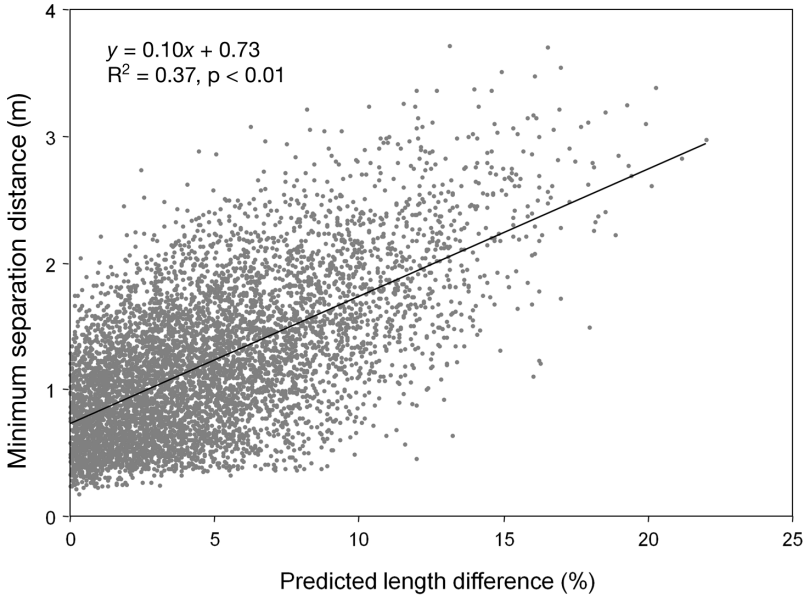

Fig. 9. *Dosidicus gigas.* The minimum separation observed between 2 adjacent individual targets in a group as a function of the predicted difference in their length

squid could be tracked acoustically are the focus of the remainder of the analyses presented. It is not clear from our observations what the function of the much larger, high-density aggregations might be, as it does not appear from our observations that *Dosidicus gigas* is a truly obligate schooler like *I. illecebrosus* (Mather & O'Dor 1984). Solitary individual squid were detected throughout all cruises, primarily at depth over deep water both night and day.

A large number of 4D acoustic tracks (e.g. Figs. 2 & 8) were isolated from the 4 sampling periods. Individual tracks showed no significant change in target strength even with changes in orientation that presumably altered tilt and roll of the individual, suggesting that the source of scattering is omnidirectional. More importantly for this work, this result confirms the use of target strength for estimating squid mantle length under a variety of conditions. This is further supported by the positive, linear, nearly one-to-one relationship between the length of squid predicted acoustically and those captured at the same location at around the same time.

Swimming speed

Over each individual track detected, the vertical velocity measured averaged 2.3 m s^{-1} (Fig. 7a). This compares well with the upper end of velocities measured using archival tags attached to large individual squid averaged over equivalent distances (e.g. 10 m) of between 0.9 to 2.6 m s^{-1} (Gilly et al. 2006, Bazzino et al. 2010). Average velocity measured using active acoustics did not vary with squid mantle length, suggesting that the measurements made using tags may apply more generally to smaller jumbo squid as well. The fact that average velocities during these coordinated upward movements are so consistent across a wide range of squid sizes suggests that the observed speeds are important to the underlying behavior, presumably foraging.

Maximum velocities measured were dramatically higher than the average velocities, with large individuals approaching 30 m s^{-1} for short time periods (3 to 5 detections; 0.3 to 1.0 s; Fig. 7b). Although the short time intervals over which these speeds were measured could introduce errors into the measurements, the significant positive relationship between the length of an individual and the maximum velocity measured during its track clearly indicates that jumbo squid can achieve very high speeds that scale with body length. The burst speeds of large individuals are comparable to fast, similarly sized teleosts like billfish (Sambilay 1990) but are roughly an order of magnitude greater than the highest vertical velocities measured with archival tags. This is likely because the sampling rate achieved using active acoustics was 5 to 10 Hz, substantially greater than the 1 Hz of the electronic tags, which enhances the capture of short events. Probably more importantly, the measurements presented here include the horizontal component of velocity whereas tags can only measure the vertical component. If only the vertical component of velocity was measured from tracks presented here, the maximum values would approach 4 m s^{-1}, much closer to maximum values measured with archival tags.

A stereotyped foraging pattern?

The overwhelming majority of squid tracks detected in this study were primarily upward in their trajectory. The upward components of these tracks showed a characteristic pattern of straight, moderate-rate swimming punctuated by erratic swimming in several areas of high use along each track (see Figs. 2 & 3). The high-use kernels had an angle be-

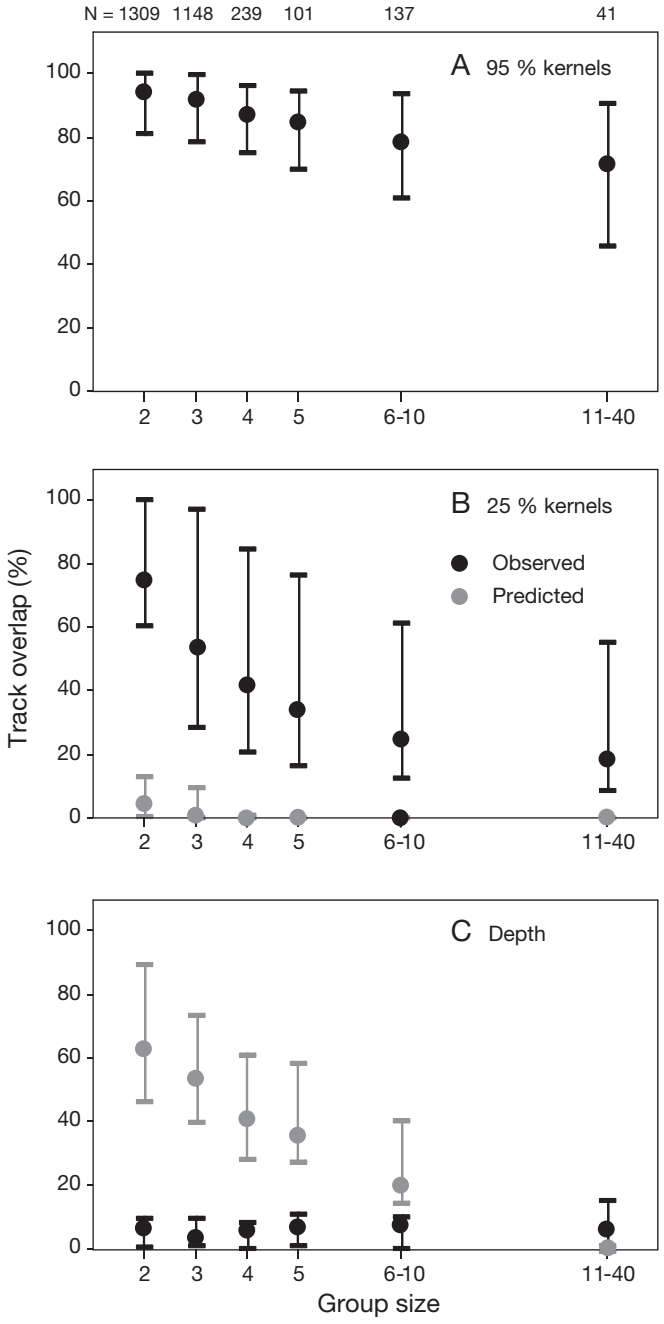

Fig. 10. *Dosidicus gigas*. The overlap between individuals in a group as a function of group size. (A) The observed overlap of all of the 95% kernels of all tracks in the group. (B) The overlap of all of the 25% kernels for a group. These values are significantly higher than chance. (C) The vertical overlap of the 25% kernels defined in the horizontal plane. The vertical overlap is significantly lower than expected by chance, remaining relatively constant regardless of group size. The number of groups analyzed in each size range is indicated along the top. For each plot the dot represents the median while the whiskers show the 95% confidence interval. Black symbols show the observed distributions. For overlap of the 25% kernels (Panels B and C), gray symbols show the predicted overlaps for squid randomly distributed over the 95% kernel for the entire group

tween them between 40° and 180° with broad modes around 60° and 180° (Fig. 6c). Thus, high-use areas in the 3D track defined vertices that were connected by straight-line swimming, resulting in an ascending, spiral-like trajectory with a triangular footprint. The size of the entire track, described by the equivalent circular diameter of the 95% density kernel, was consistently about 3.5 m, regardless of the size of the individual squid (Fig. 5a) or the depth of detection. Given the target detection characteristics employed, the width of all tracks was smaller than the footprint of the transducer's effective beam width at 3 m, where the footprint was 7 m, and deeper.

Each squid spent much of the track in several small areas, defined by the 25% kernel density. The mode size of these areas was 0.5 m in diameter (Fig. 5b) with a distance between their centroids of approximately 3 m, nearly the same as the diameter of the entire track (Fig. 5c). The behavior of the squid in these high-use kernels was quite different from the remainder of the track. First, the turning angle between adjacent detections within the 25% kernels had modes at 0°, indicating straight-line swimming, and 180°, suggesting back-and-forth motion that maintained residence within the kernel (Fig. 6a). Second, high tortuosity values measured in the 25% kernels support the interpretation of retentive swimming patterns in these areas. In contrast, movements outside the 25% kernels showed a unimodal distribution in turning angle consistent with essentially straight-line swimming (angle of 0°; Fig. 6b). Tortuosity values close to 1, meaning that the squid swam exactly as far as necessary to connect 2 points, support this.

While vertical velocity did not vary between the 95% and 25% kernel of each track, horizontal and thus 3D velocities varied significantly between these parts of the track. The 25% kernels also had significantly higher variance (standard deviation) in both horizontal and 3D velocities than the remainder of the track. This pattern is clearly evident in Fig. 3. The straight sections of the track had moderate velocities that did not vary much, whereas the parts of the track within the 25% kernels had both the highest and lowest velocities measured and very high tortuosity values. These patterns in velocity and tortuosity, together with a mode in turning angle of 180° within these high-use areas, indicate a change in swimming strategy. Turning angles of 180° are not possible in 0.2 s in a 1 m or longer individual unless the individual is reversing course. Squid predominantly swim and jet tail first but must capture prey swimming head first (Nicol & O'dor 1985). Another species of squid, *Illex illecebrosus*, feeding on swarms of eu-

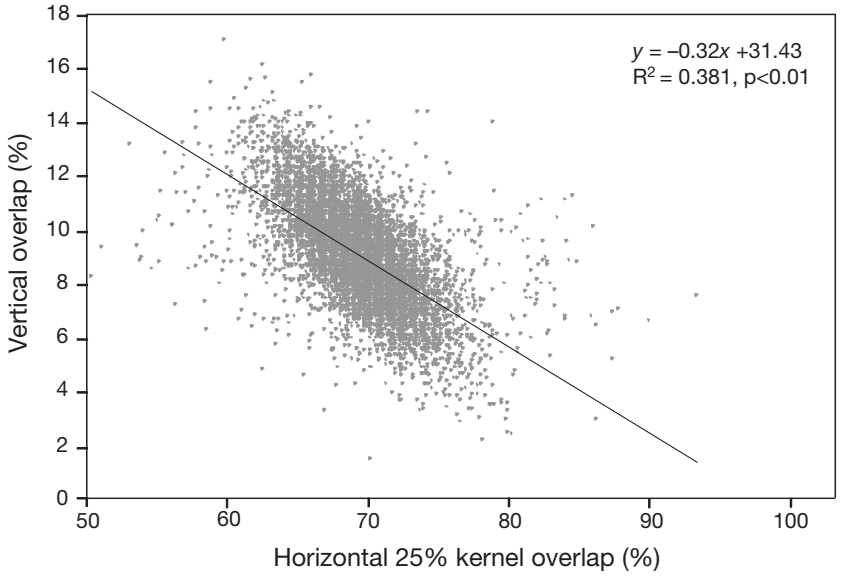

Fig. 11. *Dosidicus gigas.* Horizontal versus vertical overlap of the 25% kernels of adjacent pairs of tracks in groups with more than 4 individuals

phausiids, was observed to swim head first to attack prey but to jet tail first out of the swarm after each attack (Nicol & O'dor 1985). These visual observations of *I. illecebrosus* are consistent with the patterns in dramatic turning angle and rapid velocity alternations observed acoustically here. This rapidly changing behavior, carried out largely in the horizontal direction, would not have been resolved by the archival tags in previous studies of locomotion in free-swimming *Dosidicus gigas*.

These observations within the 25% kernels suggest that the unique behaviors within these portions of each track represent active attacks on prey. These high-use areas were separated by a horizontal distance of 3 m, on average, but this distance between high-use areas decreased when squid were feeding on euphausiids instead of fish or other prey types. When feeding on euphausiids, the 25% kernels also became smaller and the squids' velocity within the 25% kernels decreased. This indicates that the size and spacing of the high-use areas of squid tracks may reflect the distribution and/or swimming speed of the potential prey. We hypothesize that foraging may become ineffective at a given location after several attempts by a squid, and a new portion of the prey patch must therefore be exploited. As fish are more capable swimmers than euphausiids, squid may need to swim a greater distance when foraging on fish than on euphausiids to reach prey unaffected by the previous attempt and may need to swim at greater velocities during prey capture attempts. However, as 25% kernels are consistently spaced for each prey type, it appears that prey or patches of prey are relatively evenly distributed over the depth of the squid's track.

It is interesting that so many of the observed tracks were upward as squid must have been returning to deeper water after these upward excursions. Otherwise, large numbers of squid would have been collecting in shallow water during the observations: a pattern that was not observed as the largest numbers of squid were always at depth throughout each stationary period. In the observed tracks, any downward components occurred at the end of the tracking observation. These downward segments of tracks had very high vertical velocities, low tortuosity values (e.g. limited turning), and relatively shallow trajectories relative to the surface; the tracked squid thus left the echosounder beam shortly after the onset of this behavior. None of the behaviors observed on upward swimming trajectories that could be indicative of increased search effort or foraging were observed during downward swims. Downward motion may serve not only to allow the squid to return to depth, but also to relocate horizontally, allowing individuals to encounter fresh prey patches.

It should be noted that the frequency of observed upward spirals trajectories described here may have been influenced by the presence of the stationary vessel, particularly its lights. However, these swimming patterns were observed immediately at occupation of stations and during slow moving transects that permitted tracks to be observed for short periods. They were also observed on many nights during which the vessel was allowed to drift or was anchored with only relatively dim red and green running lights illuminated, suggesting this behavior occurs over a range of conditions.

Coordination of individuals within a group

About one third of detected tracks were found to parallel other simultaneously detected tracks in depth. Up to 40 individuals were simultaneously tracked. However, given the beam pattern and the distribution of tracks within it, it is likely that these large groups represent a subset of the squid exhibiting these behaviors in the area. It appears that squid in these groups are in a repeated arrangement that

forms a sort of latticework, sometimes described in schooling fish to look like crystal lattices in which individuals assume preferred positions and orientations relative to their neighbors (Parrish et al. 2002). Individually, the tracks that made up these groups looked much like individual tracks observed alone. The squid observed alone and those in groups also had a similar distribution of mantle length. There were no differences in the characteristics measured within the 25% kernels in solitary or grouped tracks, suggesting that this part of the track where prey attack and capture are likely occurring is conserved across a range of conditions. However, the tracks found in groups had lower overall tortuosity values, straighter segments between the 25% kernels, slower horizontal and faster vertical velocities, and had a smaller overall footprint than those shown by squid swimming alone. Tracks in groups may be more constrained in their overall motion because of the presence of neighbors moving in the same volume.

Adjacent individuals in groups maintained a separation distance of a least 0.25 m, and on average 1 m, throughout the duration of tracking. Fish schools can often be described by nearest-neighbor distances that are related to mean body length (Partridge 1982) and flock and school characteristics are reported and modeled in units of body length (Reynolds 1987). Typical values of packing are between 0.6 and 1.2 individuals per cubic body length (Pitcher & Partridge 1979). Using this range of densities, the spacing between individual squid of the sizes we sampled would be expected to be between 0.05 m and nearly 1.7 m. This range includes ~75% of the measured nearest-neighbor distances. However, there was no significant effect of acoustically measured squid mantle length on the spacing between individuals as predicted even though the range of individual mantle lengths covered more than 80 cm. While the percentage difference in length between the largest and smallest squid measured was 95%, squid within a group always had mantle lengths within 20% of each other and most often, within 10% of each other. Experimental work suggests that, with the number of echoes obtained from each tracked individual here, quantification of a 5% difference in length is reasonable (data from Benoit-Bird et al. 2008), so length differences of <5% should be considered statistically indistinguishable. This narrow range of sizes within a single group is consistent with observations of fish schools that are frequently segregated by size so that neighboring individuals are nearly identical (Breder 1951, Pitcher et al. 1985), reducing the individual risk of predation (Theodorakis 1989).

Despite the relatively narrow range of individual lengths within a group, there was a significant, measurable effect of the difference in length between adjacent individuals on the spacing between them (Fig. 9). Clearly, the size of an individual relative to others in the group affects the costs and benefits the individual experiences. Both the narrow range of sizes within a group and the increased spacing between individuals as their size difference increased may reflect the high levels of cannibalism that have been reported in this species, with smaller individuals being more prone to cannibalism by larger ones (Markaida et al. 2008). Perhaps even a relatively small size differential increases the risk of cannibalism for the smaller individual, necessitating an increased separation distance. The pattern in spacing observed here for squid does not fit existing models for individual spacing in fish schools (Reynolds 1987) that do not include this additional risk factor. Nor does it coincide with observations of another squid species showing a pattern inverse to that predicted by these models, with individuals getting closer together as they become larger (Hurley 1978).

Functional value of squid schooling

In addition to individuals maintaining separation throughout their tracks, there is other evidence of coordination amongst simultaneously detected tracks. Not only do tracks parallel each other in depth over time, the tracks cover the same space horizontally as measured by the 95% kernels (Fig. 10, top panel). On average, the 95% kernels of groups of up to 5 individual tracks overlapped by more than 90%. Even groups of 40 individuals had overlaps of the 95% kernels of all tracks that were greater than 50%. As highlighted in the examples in Figs. 2 & 8, high-use areas (25% kernels) of each individual track were also in the same horizontal location (Fig. 10, middle panel). For all group sizes, this overlap was much higher than predicted by chance. Although the high-use areas overlapped in horizontal space, even in large groups, these high-use areas did not overlap in vertical space (Fig. 10, bottom panel). Regardless of group size, the vertical overlap of high-use areas remained constant at around 5 to 10%. This separation in vertical space strongly suggests that adjacent individuals were each exploiting undisturbed portions of the prey field. Such coordination of horizontal positions may maximize access by individual squid to these fresh patches while allowing individuals to keep the distances connecting undisturbed areas

short. The importance of separation of high-use areas while maintaining close spacing between them is supported by the inverse relationship observed in the overlap of the 25% kernels in the horizontal and vertical planes (Fig. 11). The spacing and coordination of high-use areas within a group suggests that in order for all members of the group to benefit, prey must be relatively uniformly distributed over the volume covered by the group. A relatively uniform distribution in prey is not unexpected, at least for euphausiids and myctophids that generally form extensive layers. However, we found the same overall separation pattern in squid tracks in individuals that had been feeding primarily on myctophids, euphausiids, other fish, as well as other prey.

Despite the high degree of coordination between tracks in groups, the similarities between tracks found alone and those found in groups suggest that the upwardly spiraling swimming path punctuated by periods of back-and-forth swimming at the vertices has a similar function in both cases. The size of the group tracked was directly proportional to the density of squid found in the dense aggregation below the tracked individuals. Grouping of tracks appears to be an indirect effect of the local individual density rather than a specific tactic. While there may be adaptive reasons for the dense aggregations observed below the tracks, the high levels of coordination observed between individuals in the smaller, tracked groups are likely driven by the need to maintain separation in these ascending forays. There is no evidence that grouping in squids confers a direct foraging benefit as in the case of cooperation, though there may be other benefits.

Acoustically collected, 4D spatio-temporal data revealed that individual squid are moving relative to each other with dramatic changes in orientation and behavior in a short period of time, likely in order to forage on potential prey that were found at the same depths. Despite this, these squid are maintaining a coherent, patterned structure within each group, consistent with the definition of schooling (Norris & Schilt 1988). These patterns would have been difficult, if not impossible to identify from static observations of these squid. Polarization within groups did not break down during apparent feeding events, characterized by repeated back-and-forth swimming in small, horizontally correlated but vertically separated locations. Breakdown of schooling during prey chase and capture has been observed in other foraging squid (Foyle & O'Dor 1988), euphausiids (Hamner et al. 1983), and many schooling fish species (Pitcher & Parrish 1993, DeBlois & Rose 1995, Ryer & Olla 1998). In contrast, in jumbo squid foraging in shallow water at night, it appears that the feeding events themselves may anchor the group.

The ability to track individual squid in 4 dimensions, albeit for short durations, allowed us to describe aggregations of squid mechanistically, a key step for testing hypotheses to explain aggregation in animals. The 2 distinct types of aggregations found simultaneously in jumbo squid appear to have very different functions as well as cost–benefit tradeoffs. Further exploration of these patterns will provide an opportunity to test hypotheses about shoaling and schooling that have primarily been developed from studies of fish. That jumbo squid frequently exhibit social behaviors — being in groups that show highly polarized, complex, coordinated movement patterns — is likely critical for understanding many aspects of their biology, estimating their standing stock biomass, and predicting the impacts of the fishery that they support and on others that they prey on. Descriptions of schooling behavior in this large marine invertebrate, a group not well represented in the schooling literature, provide an important point for comparative analyses of group living.

Acknowledgements. W. Au, L. Bell, A. Booth, S. Bush, D. Cade, T. Chesney, P. Daniel, A. Fleishman, S. Hafker, E. Hogan, L. Irvine, N. McIntosh, H. Rosen, D. Shulman, J. Schneider, A. Stoehr, K. Storey, T. Towanda, T. Uyeno, B. Velleco, C. Waluk, and I. Wilson provided assistance in the field. U. Markaida and J. Ramos made determinations of sexual maturity stage and stomach contents. C. Waluk conducted preliminary acoustic analyses. A. Kaltenberg provided constructive feedback on an earlier draft of the manuscript. B. Anderson-Becktold, C. Pekar, and C. Salinas and his students from Centro de Investigaciones Biológicas del Noroeste (CIBNOR) provided logistical support. B. Mate and the Oregon State University Marine Mammal Institute provided vessel time and support for the 2007 cruise while Captain B. Pedro and Engineer W. Schlecter provided assistance both in preparation for and during that cruise. The captains and crews of the RV 'BIP XII' and RV 'New Horizon' provided valuable support during later cruises. B. Seibel was a collaborator and Chief Scientist on the 2010 and 2011 cruises. This work was supported by grants from the National Science Foundation (OCE0851239 to K.J.B.-B. and OCE0526640/0850839 to W.F.G.) and the David and Lucile Packard Foundation.

LITERATURE CITED

Bazzino G, Gilly WF, Markaida U, Salinas-Zavala CA, Ramos-Castillejos J (2010) Horizontal movements, vertical-habitat utilization and diet of the jumbo squid (*Dosidicus gigas*) in the Pacific Ocean off Baja California Sur, Mexico. Prog Oceanogr 86:59–71

Benoit-Bird KJ, Gilly WF, Au WWL, Mate BR (2008) Controlled and in situ target strengths of the jumbo squid *Dosidicus gigas* and identification of potential acoustic scattering sources. J Acoust Soc Am 123:1318–1328

Bertram B (1978) Living in groups: predators and prey. In: Krebs JR, Davies NB (eds) Behavioural ecology: an evolutionary approach. Blackwell Scientific Publications, Oxford, p 64–96

Blackman S (1986) Multiple-target tracking with radar applications. Artech House, Dedham, MA

Breder CMJ (1951) Studies on the structure of fish shoals. Bull Am Mus Nat Hist 98:1–27

Campbell DJ (1990) Resolution of spatial complexity in a field sample of singing crickets *Teleogryllus commodus:* a nearest-neighbor analysis. Anim Behav 39:1051–1057

DeBlois E, Rose G (1995) Effect of foraging activity on the shoal structure of cod (*Gadus morhua*). Can J Fish Aquat Sci 52:2377–2387

Foote KG, Vestnes G, Maclennan DN, Simmonds EJ (1987) Calibration of acoustic instruments for fish density estimation: a practical guide. ICES Coop Res Rep 144

Forsythe J, Kangas N, Hanlon RT (2004) Does the California market squid (*Loligo opalescens*) spawn naturally during the day or at night? A note on the successful use of ROVs to obtain basic fisheries biology data. Fish Bull 102: 389–392

Foyle TP, O'Dor RK (1988) Predatory strategies of squid (*Illex illecebrosus*) attacking small and large fish. Mar Behav Physiol 13:155–168

Gilly WF, Markaida U, Baxter CH, Block BA and others (2006) Vertical and horizontal migrations by the jumbo squid *Dosidicus gigas* revealed by electronic tagging. Mar Ecol Prog Ser 324:1–17

Hamner WM, Hamner PP (2000) Behavior of Antarctic krill (*Euphausia superba*): schooling, foraging, and antipredatory behavior. Can J Fish Aquat Sci 57:192–202

Hamner WM, Hamner PP, Strand SW, Gilmer RW (1983) Behavior of Antarctic krill, *Euphausia superba*: chemoreception, feeding, schooling, and molting. Science 220: 433–435

Handegard NO, Patel R, Hjellvik V (2005) Tracking individual fish from a moving platform using a split-beam transducer. J Acoust Soc Am 118:2210–2223

Hanlon R (1998) Mating systems and sexual selection in the squid *Loligo*: How might commercial fishing on spawning squids affect them? CalCOFI Rep 39:92–100

Hanlon RT, Hixon RF, Forsythe JW, Hendrix JP Jr (1979) Cephalopods attracted to experimental night lights during a saturation dive at St. Croix, US Virgin Islands. Bull Amer Malacol Union 1979:53–58

Hurley A (1978) School structure of the squid *Loligo opalescens.* Fish Bull 76:433–442

Lipinski MR, Underhill L (1995) Sexual maturation in squid: Quantum or continuum? S Afr J Mar Sci 15:207–223

Magurran A, Oulton W, Pitcher T (1985) Vigilant behaviour and shoal size in minnows. Z Tierpsychol 67:167–178

Markaida U, Gilly WF, Salinas-Zavala C, Rosas-Luis R, Booth A (2008) Food and feeding of jumbo squid *Dosidicus gigas* in the central Gulf of California during 2005–2007. Calif Coop Oceanic Fish Invest Rep 49

Mather JA, O'Dor RK (1984) Spatial organization of schools of the squid *Illex illecebrosus.* Mar Behav Physiol 10: 259–271

Moltschaniwskyj NA, Pecl GT (2007) Spawning aggregations of squid (*Sepioteuthis australis*) populations: a continuum of 'microcohorts'. Rev Fish Biol Fish 17:183–195

Morales JM, Haydon DT, Frair J, Holsinger KE, Fryxell JM (2004) Extracting more out of relocation data: building movement models as mixtures of random walks. Ecology 85:2436–2445

Nesis KN (1970) The biology of the giant squid of Peru and Chile, *Dosidicus gigus.* Oceanology 10:140–152

Nicol S, O'dor R (1985) Predatory behaviour of squid (*Illex illecebrosus*) feeding on surface swarms of euphausiids. Can J Zool 63:15–17

Norris KS, Schilt CR (1988) Cooperative societies in three-dimensional space: on the origins of aggregations, flocks, and schools, with special reference to dolphins and fish. Ethol Sociobiol 9:149–179

Okubo A (1986) Dynamical aspects of animal grouping: swarms, schools, flocks, and herds. Adv Biophys 22:1–94

Parrish JK (1991) Do predators 'shape' fish schools: interactions between predators and their schooling prey. Neth J Zool 42:358–370

Parrish JK, Turchin P (1997) Individual decisions, traffic rules, and emergent pattern in schooling fish. In: Parrish JK, Hamner WM (eds) Animal groups in three dimensions. Cambridge University Press, Cambridge, p 126–142

Parrish JK, Viscido SV, Grunbaum D (2002) Self-organized fish schools: an examination of emergent properties. Biol Bull 202:296–305

Partridge BL (1980) The effect of school size on the structure and dynamics of minnow schools. Anim Behav 28:68–77

Partridge BL (1982) The structure and function of fish schools. Sci Am 246:114–123

Pitcher TJ, Parrish JK (1993) Function of shoaling behavior in teleosts. In: Pitcher TJ (ed) Behavior of teleost fishes. Chapman and Hall, New York, NY, p 363–439

Pitcher TJ, Partridge BL (1979) Fish school density and volume. Mar Biol 54:383–394

Pitcher TJ, Magurran AE, Winfield I (1982) Fish in larger shoals find food faster. Behav Ecol Sociobiol 10:149–151

Pitcher T, Magurran A, Edwards J (1985) Schooling mackerel and herring choose neighbours of similar size. Mar Biol 86:319–322

Reynolds CW (1987) Flocks, herds and schools: a distributed behavioral model. ACM SIGGRAPH Comput Graph 21: 25–34

Ruzzante DE (1994) Domestication effects on aggressive and schooling behavior in fish. Aquaculture 120:1–24

Ryer CH, Olla BL (1998) Shifting the balance between foraging and predator avoidance: the importance of food distribution for a schooling pelagic forager. Environ Biol Fishes 52:467–475

Sambilay VC Jr (1990) Interrelationships between swimming speed, caudal fin aspect ratio and body length of fishes. Fishbyte 8:16–20

Sawada K, Furusawa M, Williamson NJ (1993) Conditions for the precise measurement of fish target strength *in situ.* Fish Sci 20:15–21

Shaw E (1978) Schooling fishes. Am Sci 66:166–175

Shchetinnikov AS (1988) Feeding and food relations of abundant squids in southeastern part of the Pacific Ocean. Autoreferat Dissertatsii na Soiskani Uchenoj Stepeni Kandidata Biologicheskikh Nauka, Moscow (in Russian with English Abstract)

Smale M, Sauer W, Roberts M (2001) Behavioural interactions of predators and spawning chokka squid off South Africa: towards quantification. Mar Biol 139:1095–1105

Theodorakis CW (1989) Size segregation and the effects of oddity on predation risk in minnow schools. Anim Behav 38:496–502

Turchin P (1991) Translating foraging movements in heterogeneous environments into the spatial distribution of foragers. Ecology 72:1253–1266

Worton BJ (1989) Kernel methods for estimating the utilization distribution in home-range studies. Ecology 70:164–168

Zeidberg L, Robison B (2007) Invasive range expansion by the Humboldt squid, *Dosidicus gigas*, in the eastern North Pacific. Proc Natl Acad Sci USA 104:12948–12950

Editorial responsibility: Nick Tolimieri, Seattle, Washington, USA

Submitted: November 14, 2011; Accepted: February 2, 2012
Proofs received from author(s): May 5, 2012